ISBN: 978-3-95450-247-9 ISSN: 2673-5490 doi: 10.18429/JACoW-IPAC2024-THPG40

TIME-OF-FLIGHT BEAM LOSS MONITOR FOR THE ADVANCED PHOTON SOURCE UPGRADE BOOSTER-TO-STORAGE RING TRANSPORT LINE*

J. Dooling, A. Brill, J. Liu, S. Shoaf, S. Wang
Argonne National Laboratory, Lemont, IL 60439, USA

Abstract

We present initial results from the booster-to-storage ring beam-loss montior (BTS BLM) employing time-of-flight analysis to localize and minimize losses along the BTS line. The BTS BLM utilizes a pair of high-purity, fused-silica fiber optic cables running in parallel along the 65-m BTS transport line. Photomultipliers located at both upstream and downstream ends of each fiber monitor Čerenkov radiation generated by lost electrons. The downstream detectors receive temporally compressed, higher-intensity, spatially inverted signals, while the upstream waveforms are temporally expanded with lower intensity allowing finer time resolution; both upstream and downstream effects owing to the refractive index in the fiber glass. Each radiation-hardened optical fiber is composed of 600, 660, and 710-micron-diameter core, cladding, and buffer, and is similar to those used in the newly commissioned LCLS-II superconducting linac BLM system. Real-time waveforms are recorded on a fast oscilloscope and available for diagnostic observation through EPICS waveform records. Remote controlled high-voltage power supplies provide gain adjustment. Data from booster and storage ring commissioning are presented.

INTRODUCTION

The Advanced Photon Source Upgrade (APS-U) booster-to-storage ring (BTS) transfer line transports full-energy, 6-GeV electrons for injection into the newly installed, fourth-generation storage ring (4GSR). The new BTS line differs from the former due to the addition of emittance-exchange optics transversely rotating beam properties from horizontal to vertical and vice versa. Beam loss is a concern due to multiple variations in aperture along the line. The BTS line also includes an emittance exchange section to improve injection efficiency. Employing high-purity, fused-silica (rad hard) optical fibers, high-energy electron beam loss is detected via Čerenkov radiation. These beam loss monitors (BLMs) use time-of-flight (TOF) analysis to identify loss positions along the BTS line. The BTS BLM TOF (BBT) system is purely a diagnostic one unlike the Beam Containment System installed at SLAC, which provides machine protection [1].

ANALYSIS

Photomultiplier tubes (PMTs) are placed at both the upstream (US) and downstream (DS) ends of each fiber. Signal intensity from distributed losses along a given fiber will differ between US and DS locations. Spatially distributed loss in a given fiber will appear with different temporal profiles at each end. The BBT diagnostic is presented schematically in Fig. 1. We can compare the expected spatial resolution for the US and DS positions. Referring to Fig. 1, the time for a signal generated at loss positions 1 and 2 to reach the oscilloscope from the US location may be written as,

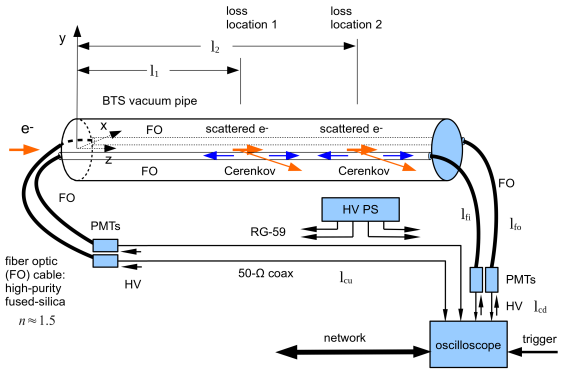

Figure 1: BTS BLM TOF (BBT) diagnostic schematic.

$$t_{1u} = \frac{l_1}{v_f} + \frac{l_{cu}}{v_c} \quad (1)$$

$$t_{2u} = \frac{l_2}{v_f} + \frac{l_2 - l_1}{c} + \frac{l_{cu}}{v_c}, \quad (2)$$

where $v_f = c/n_f$ with n_f the index of refraction. and v_c is the propagation velocity in the coax cable. The time difference

$$\Delta t_u = t_{2u} - t_{1u} = \frac{(l_2 - l_1)(c + v_f)}{c v_f} = \frac{l_2 - l_1}{c}(n_f + 1). \quad (3)$$

For the DS location, the times for loss signals from positions 1 and 2 become

$$t_{1d} = \frac{l_c - l_1}{v_f} + \frac{l_{cd}}{v_c} \quad (4)$$

$$t_{2d} = \frac{l_c - l_2}{v_f} + \frac{l_2 - l_1}{c} + \frac{l_{cd}}{v_c}, \quad (5)$$

and the time difference

$$\Delta t_d = t_{2d} - t_{1d} = -\frac{(l_2 - l_1)(c - v_f)}{c v_f} = -\frac{l_2 - l_1}{c}(n_f - 1). \quad (6)$$

Eqation (6) shows the distributed loss signals observed on the DS detectors are time-reversed. The spatial resolution for

* Work supported by the u.s. department of energy, office of science, office of basic energy sciences, under contract number de-ac02- 06ch11357.

ISBN: 978-3-95450-247-9 ISSN: 2673-5490 doi: 10.18429/JACoW-IPAC2024-THPG40

US and DS detectors may be calculated assuming a minimum time response for the system, Δt_r. Redefining $(l_2 - l_1) \rightarrow \Delta s$, we can write

$$\Delta s_u = \frac{c\Delta t_r}{n_f + 1} \tag{7}$$

$$\Delta s_d = \frac{c\Delta t_r}{n_f - 1}. \tag{8}$$

The ratio of Eqs. (7) and (8) yields

$$\frac{\Delta s_u}{\Delta s_d} = \frac{n_f - 1}{n_f + 1} = 0.2, \tag{9}$$

for $n_f = 1.5$. Thus the spatial resolution for the US detector is a factor of 5 better than for the DS. For equal numbers of photons with identical spectra traveling US and DS along the fiber, Eqs. (7) and (8) imply the DS signal will be 5 times greater than the US. This simple model ignores the dispersive effects in the coaxial cables where higher frequencies will suffer greater attenuation [2]. We can let $\Delta s \rightarrow ds$ and $\Delta t \rightarrow dt$ and write

$$ds_d = -\frac{c}{n_f - 1} dt_d \tag{10}$$

$$ds_u = \frac{c}{n_f + 1} dt_u. \tag{11}$$

Čerenkov radiation and the PMTs chosen (Hamamatsu R7400U-04) favor the blue end of the visible spectrum; therefore, the index of refraction at 400 nm is employed for calculations; here $n_f = 1.47$ [3].

EXPERIMENTAL DESCRIPTION

The BBT consists of two optical fibers running roughly at beam elevation on opposite sides of the transport line shown in Fig. 2. The fibers run from the AQ1 quadrupole in the booster tunnel to the DQ2 quadrupole in the SR. The fiber cross sections are 600, 660, 710, and 2000 μm for core, clad, polyimide, and outer jacket diameters, respectively.

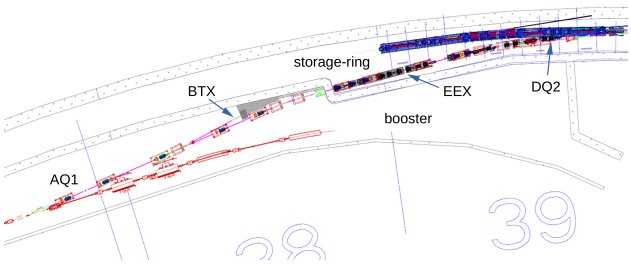

Figure 2: Booster-to-storage ring (BTS) line. The fiber optic cable runs from the AQ1 magnet on the booster side to the DQ2 magnet in the storage ring (SR). The cables run through the shielded penetration between the tunnels as well as the emittance exchange section (EEX) in the SR. The booster-to-dump (BTX) line leads to the booster dump.

The fibers thread through and around various elements in the BTS line, including quadrupoles, as seen in Fig. 3. In addition, leveled 3-D-printed mounts held the fiber optic (FO) cable to open sections of the beamline. The minimum bending radius specified for the FO cable is 20 cm. Waveforms from the PMTs were recorded using a networked Teledyne Lecroy 9254M Waverunner oscilloscope.

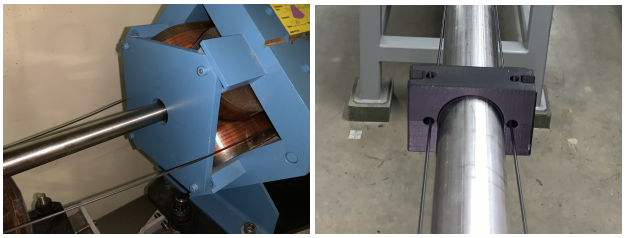

Figure 3: Left: BLM FO cables running through a BTS quadrupole. Right: 3-D-printed mounts hold the FO cables close to open sections of the BTS beamline.

MEASUREMENTS

Without Beam

For the TOF measurements, the electrical lengths of both coax and fiber cables are required. Coax cable delays were measured using an Agilent Infinium DCA-J 85100C Digital Communications Analyzer and are listed in Table 1. With cable propagation speed given as $v_c = 0.83c$, lengths are calculated as $l_c = t_d v_c/2$. Coax cable lengths differed considerably between US and DS runs.

Table 1: RF Coaxial Cable Lengths

Channel No.	Location	Delay t_d (ns)	l_c (m)
1	US,in	370.81	46.134
2	US, out	377.25	46.935
3	DS, in	541.13	67.324
4	DS, out	540.82	67.286

The FO cables were measured from the DS detector location (SR) splitting a 20-ns rectangular pulse between one of the DS signal cables and a short piece of coax cable ($l_{cs} = 1.98$ m) terminated with an LED. The LED was then directly coupled to one of the two PMTs. Delays measured on the oscilloscope, t_{ds}, of 222.7 ns and 225.4 ns were observed on the inboard and outboard cables, respectively. Employing the data from Table 1,

$$t_{dd} + t_{ds} = \frac{l_{cs}}{0.83c} + t_f + t_{du}. \tag{12}$$

Rearranging with $t_f = l_f/v_f = n_f l_f/c$, we find for l_f,

$$l_f = \frac{c}{n_f}\left(\frac{t_{dd}}{2} + t_{ds} - \frac{l_{cs}}{0.83c} - \frac{t_{du}}{2}\right). \tag{13}$$

For the inboard and outboard fibers, Eq. (13) yields 61.16 m and 61.02 m, respectively. These lengths are consistent with installed values.

ISBN: 978-3-95450-247-9 ISSN: 2673-5490 doi: 10.18429/JACoW-IPAC2024-THPG40

With Beam

Initial APS-U commissioning BBT measurements were made with beam extracted to the booster dump along the stub BTX line (see Fig. 2). Prior to fine tuning the transport line, the signals on the four channels versus time are shown in Fig. 4. The US and DS signals are evident along with weaker reflected features. The sample interval in this case was 400 ps (rate: 2.5 GS/s). The scope was set to trigger 347.5 μs after a pre-trigger extraction/injection timing fiducial. Whereas the US channels show loss signals with varying features, the DS pulses show little variation. This result was anticipated based on the reduced resolution (increased compression) of the DS signals as expressed by Eqs. (8) and (9). Converting time to distance along the beamline by integrating Eq. (11) and overlaying the magnets' positions, we plot the US signals presented in Fig. 4 along the BTS line in Fig. 5. Dispersion is largest at quadrupoles AQ2 and AQ4, the second and fourth quads shown (quads are the taller blocks, dipoles the shorter ones).

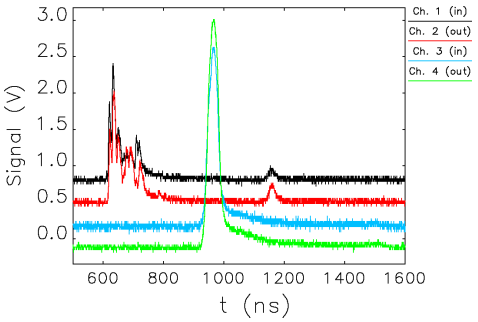

Figure 4: Initial BBT signals with beam extracted to the BTX beam dump. Waveforms are vertically offset for clarity.

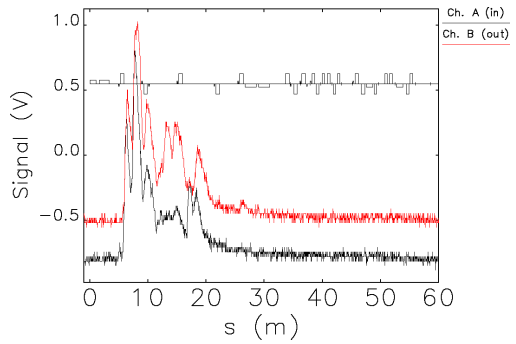

Figure 5: US BBT signals versus position along the BTS beamline with booster beam extracted to the BTX beam dump and magnet positions overlaid. The taller rectangles are quadrupoles and the shorter rectangles are dipoles. Waveforms are vertically offset for clarity.

We obtained permission to send beam to the SR on 10 April 2024 [4]. In addition to the aperture step sizes, the insertion of scintillator flags in the line provided another method to localize loss positions. Figure 6 presents the loss waveforms plotted versus position while the flag at FS4 was inserted into the beam. This takes place near s=45 m. Peaks

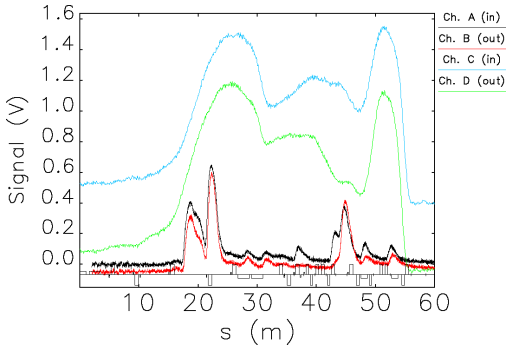

Figure 6: Loss patterns over the BTS line based on time signals from the FO cable. A flag is inserted near s=45 m.

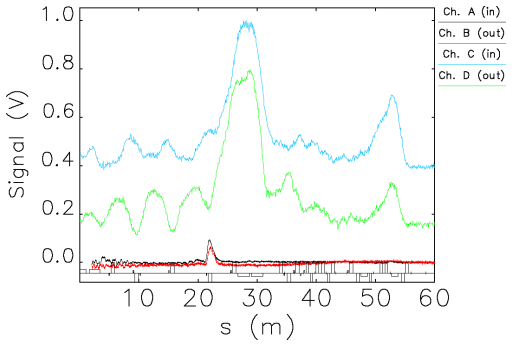

Figure 7: Loss patterns after tuning the BTS line and removing all flags. The PMT gain was increased by a factor of 17 over the case shown in Fig. 6.

further upstream are likely due to early misalignment and beam halo. After removal of the flag and tuning of the line, losses dropped significantly; Fig. 7 shows the resulting loss pattern. Here the PMT high voltage bias was raised on all four channels relative to the case in Fig. 6 from -400 V to -600 V, resulting in a 17-fold increase in gain. The gain of the PMTs may be expressed in terms of PMT charge [5] as $Q(V)/Q_{ref} = (V/V_{ref})^{n_d-1}$, where Q_{ref} is the output charge at $V = V_{ref}$, and n_d is the number of dynodes; in the present case, $n_d = 8$. The observed output voltage, $V_o = R(dQ/dt)$ begins to flatten above 1 V; however, the pulse width becomes broader so the output charge continues to increase. Here $R = 50\,\Omega$.

DISCUSSION AND SUMMARY

Fiber optic cable can provide loss locations along the BTS line, and the best resolution is obtained from the US detector location.Increased loss signal levels observed at the DS detectors are caused by compression of the loss distribution seen by the fibers as well as forward-directed electromagnetic shower from scattered high-energy electrons.

ACKNOWLEDGEMENTS

Thanks to A. Fisher of SLAC for facilitating procurement of the optical fiber. Thanks also to R. Soliday and H. Shang for assistance with analysis scripts.

ISBN: 978-3-95450-247-9 ISSN: 2673-5490 doi: 10.18429/JACoW-IPAC2024-THPG40

REFERENCES

[1] A. Fisher *et al.*, "Beam-loss detection for the high-rate superconducting upgrade to the slac linac coherent light source," *Phys. Rev. Accel. Beams*, vol. 23, no. 8, p. 082 802, 2020. doi:10.1103/PhysRevAccelBeams.23.082802

[2] J. A. Stratton, *Electromagnetic Theory*. McGraw-Hill, New York, 1941, p. 554.

[3] W. S. Rodney and R. J. Spindler, "Index of refraction of fused-quartz glass for ultraviolet, visible, and infrared wavelengths," *J. Res. Natl. Bur. Stand.*, vol. 53, p. 185, 1954.

[4] Y. Sun, private communication, 2024.

[5] J. C. Dooling, M. Borland, K. C. Harkay, R. T. Keane, B. J. Micklich, and C. Yao, "A Fast Beam Interlock System for the Advanced Photon Source Particle Accumulator Ring," in *Proc. IPAC'18*, Vancouver, Canada, Apr.-May 2018, pp. 1815–1818. doi:10.18429/JACoW-IPAC2018-WEPAF005